Blade sweep and reversibility of axial flow fan

PhD thesis

Dániel Fenyvesi

Gödöllő
2014

Doctoral school denomination: Technical Science Doctoral School

Science: Basics of Agricultural Machine Engineering

Leader: Prof. Dr. István Farkas
Dr. of Technical Sciences
Faculty of Mechanical Engineering
Szent István University, Gödöllő, Hungary

Supervisor: Prof. Dr. Ferenc Szlivka
professor, CSc
Mechatronical and Autotechnical Institution
Donát Bánki Faculty of Mechanical and Safety Engineering
Óbudai University, Budapest, Hungary

…… ……
Affirmation of the Doctoral School Leader Affirmation of Supervisor

TABLE OF CONTENTS

NOMENCLATURE

γ	blade section stagger angle measured from axial direction	[deg]
η_h	hydraulic efficiency	[-]
η_{hT}	designing hydraulic efficiency	[-]
Θ	angle of blade chord	[deg]
ΔP_t	stagnation pressure difference after and before rotor in absolute frame of reference	[Pa]
Δp_{cir}	pressure changing interpreted into circumferential direction	[Pa]
ν	hub to tip ratio	[-]
ρ	density	[kg/m^3]
σ	solidity	[-]
τ	tip clearance	[m]
φ	flow coefficient	[-]
φ_3	local axial flow coefficient	[-]
ψ	pressure coefficient	[-]
ψ_{meas}	flow coefficient originated from measure	[-]
ψ_t	designing pressure coefficient	[-]
A_{gy}	area of torus section	[m^2]
AFB	axial flow blockage	[-]
C_L	lift coefficient	[-]
C_n	discharge coefficient	[-]
C_p	static pressure coefficient	[-]
c	chord	[m]
c_a	chord at the blade tip	[m]
c_i	chord at the blade hub	[m]
c_k	chord at the midspan	[m]
DF	diffusion coefficient	[-]
DF_a	diffusion number at blade tip	[-]
DF_i	diffusion number at blade hub	[-]
DF_k	diffusion number at midspan	[-]
DF_{loc}	local diffusion number	[-]
DH	ratio of inlet- and outlet relative velocity (DE Haller number)	[-]
f_{ax}	unit function of axial flow blockage	[-]
h	blade span	[m]
J	goodness factor	[-]
k	constant of angular moment	[-]
n	exponent of angular momentum	[-]
n_f	rotor revolution	[1/s]
N	blade number	[-]
p	pressure	[Pa]

p_t	stagnation pressure at the relative frame of reference	[Pa]
p_0	static pressure before leading edge	[Pa]
p_{00}	stagnation pressure before leading edge interpreted in relative frame of reference	[Pa]
Q	volume flow	[m^3/s]
R^*	dimensionless radius	[-]
r	radius	[m]
r_i	hub radius	[m]
r_k	midspan radius	[m]
r_a	tip radius	[m]
Re	Reynolds number	[-]
s	pitch	[m]
spn	dimensionless coordinate along span	[-]
u	peripheral speed	[m/s]
u_a	peripheral speed at blade tip	[m/s]
v_0	inlet relative velocity	[m/s]
v_{3m}	outlet axial velocity project on the axial direction	[m/s]
v_{3u}	absolute circumferential velocity behind trailing edge	[m/s]
w_m, w_{ax}	relative velocity project on axial direction	[m/s]
w_r	radial velocity	[m/s]
$\boldsymbol{w}_s$	vector of secondary flow	[m/s]
w_{sb2b}	secondary velocity on designed 2D plain	[m/s]
$\overline{w}_N$	average velocity through the gap	[m/s]
$w_{N,2D}$	ideal velocity through the gap	[m/s]
$\overline{w}_{N,2D}$	ideal average velocity through the gap	[m/s]
w_0	inlet relative velocity	[m/s]
w_3	outlet relative velocity	[m/s]
w_{3b2b}	component of outlet relative velocity interpreted in designed plain	[m/s]
w_{sb2b}	outlet relative velocity perpendicular on designing plane	[m/s]
w_∞	average velocity of inlet and outlet velocity at relative frame of reference	[m/s]
$w_{\max,free}$	maximum relative velocity at the blade suction surface	[m/s]
x	coordinate	[m]
Y_r	averaged radial flow coefficient	[-]
Y_{sb2b}	averaged secondary flow coefficient	[-]
$[\bullet]_a$	value at the hub	
$(\bullet)_{CFD}$	3D viscous CFD	

$(\bullet)_{STR}$	blade of radial staking line
$(\bullet)_{SW}$	swept blade (on the hub and tip)
AFB	axial flow blockage
CVD	controlled vortex design
FV	free-vortex design
PS	pressure side
SS	suction side
STR	straight blade
SW	positive swept blade (on the hub and tip)
TLF	tip leakage flow
TLV	tip leakage vortex
VC	Vena Contracta

1. INTRODUCTION AND OBJECTIVES

1.1. Importance of the chosen thesis

Application of fans in the field of agriculture and industry is very multiplex: airing in animal raising settlements and greenhouses, technological processes of refrigerating plants, drying devices, powder-separating and power plant. A modern ventilation system can have an influence on competitiveness of some agricultural and industrial units. Developing blade rotors can contribute to the economic function.

In the case of improving rotor blade design and for better understanding fluid flow processes in interblade we need get acquainted with 3D-flow processing. For analyzing the 3D flow particularly the main interblade flow phenomena have to be localized like occurrences of hub-separating, tip leakage flow, wall boundary layer flow. During the design flow rate there common interaction has on effect on angular momentum that is hydraulic efficiency of blade row. My aim is to create such a calculating model which can take the above mention loss parameters into consideration and it can estimate their effect during preliminary design. Parameters of preliminary design in the case of this way combined blade geometry are consequences of the monitoring and investigating fluid-flow parameters. According to this the new calculating model needs modern CFD technics and an iterative approaching for goodness-decision.

Synchronized with the above mention facts I have a further aim to investigate the planning parameters and regulablity of flat plate bladed rotor with simple geometry. With application of flat plate blade reversibility can be realized, can become possible. Such simple ventilator construction must be suitable for fulfilling tasks within agricultural airing, for eg. in the case of agricultural produce storing and drying because of the need of bi-directional flow.

1.2. Aims and goals

My aims are the followings:

1. 3D numerical investigation of the rotor designed on controlled vortex deign (CVD) in the case of different blade leakage.
2. Creating a calculating model based on controlled vortex design method, can usually cause swept blades and takes the 3D interblade flow phenomena into consideration during the preliminary design. My further aim is the comparing investigation rotors with the new calculating model in spite of traditional straight-stacking-line blade.
3. Designing reversible axial flow fan with simple geometry flat plate blade and analyzing of characteristic.

2. MATERIAL AND METHODS

2.1. Rotor calculating with the help of constant chord method, preliminary design

The preliminary design calculates the straight bladed reference cascade. With the application of controlled vortex design can become possible to choose angular momentum distribution, in order that blade chord remains constant at the radii. During the calculation the absolute tangential velocity is the following:

$$v_{3u} = k \cdot r^n \tag{2.1}$$

I calculate velocity triangles with the help of (2.1) and radial equilibrium equation.

With full knowledge of velocity triangles I calculate the stagger angle camber angle of blade profile camber line according to McKenzie (1997). Starting parameters of the calculation can be found in the Table 2.1.

Table 2.1: Nominal design data of Dan26-STR rotor

Parameter	**Value**
Flow coefficient (φ)	0.5
Pressure coefficient (ψ)	0.6
Revolution (n_f)	1200 min^{-1}
Outer radius (r_a)	315 mm
Blade number (N)	12
Hub to casing ratio (ν)	0.676
Designed hydraulic efficiency (η_{hT})	0.9
Constant diffusion number (DF)	0.5
Blade profile	C4-10%

Necessary data of geometrical construction for calculated are summarized in the Table 2.2.

Table 2.2: Geometrical parameters of Dan26-STR

	Hub	**Midspan**	**Tip**
Blade chord, (c) [mm]	109	109	109
Camber angle, (Θ) [deg]	32.3	28.5	27.1
Stagger angle, (γ) [deg]	41.9	48.4	52.9

2.2. Swept blade design with prescribed diffusion factor method

At constructing swept blade I have chosen the less designing diffusion number keeping angular distribution along the span of referent blade row on the section of blade hub and blade tip. The lesser diffusion number result in greater chord compared to reference blade constant chord.

The place of trailing edge in the case of sections remain original. The Figure 2.1 represents the stacking method which results swept blade form. The stagger angle remains unchangeable according to reference (STR). Harmonizing with it the sections of blade ends are positive swept (+SW). In my thesis the stacking line means the midpoint-matching bow of blade camber length of arch.

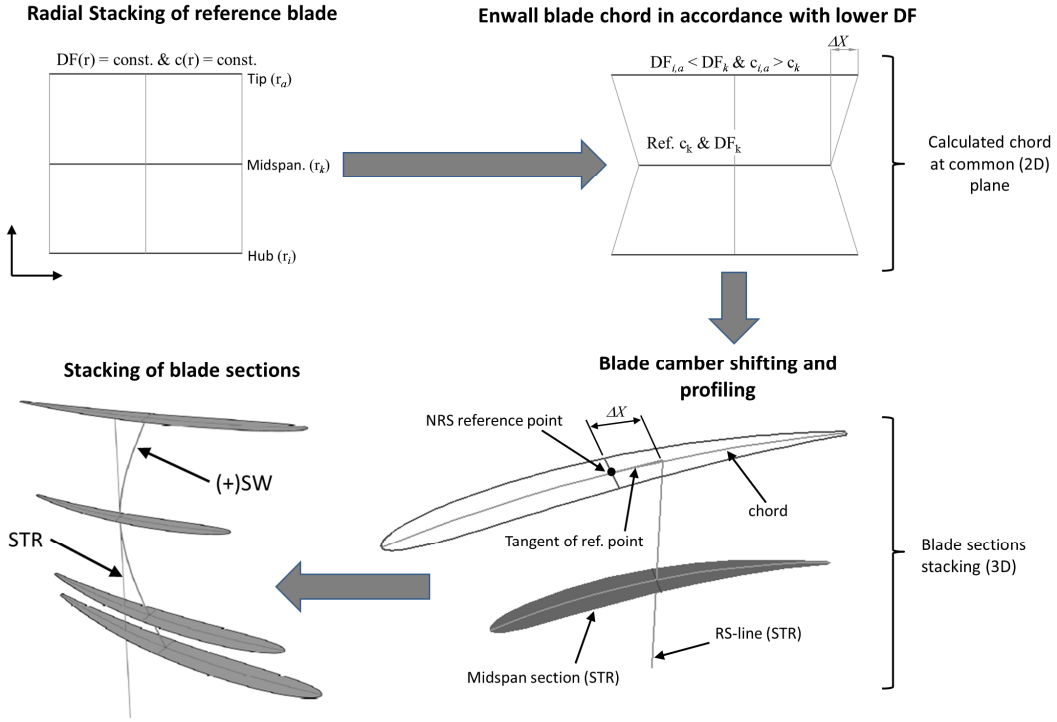

Fig. 2.1.: Stacking of swept blade

At increasing of designed diffusion number of blade ends the changing of hydraulically achievement has to bee taken into consideration. It can be characterized with introducing of Goodness-Factor:

$$J = \frac{2\pi}{Q}\int_{r_i}^{r_a} \frac{\Delta P_{t(SW)}(r)}{\Delta P_{t(STR)}(r)} \cdot v_{3m(STR)}(r)\, r dr \qquad (2.2)$$

In my thesis the main parameter of the investigated swept blade row (Dan26-SW) are represented in the Table 2.3.

Table 2.3: Geometrical parameters of Dan26-SW blade row

	Hub	Midspan	Tip
Designing diffusion number (DF)	0.454	0.5	0.438
Chord, (c) [mm]	143.3	109	143.3
Camber angle, (Θ) [fok]	27.2	28.5	22.3
Stagger angle, (γ) [fok]	41.9	48.4	52.9

Views of designed Dan26-SW swept blade (Figure 2.2.).

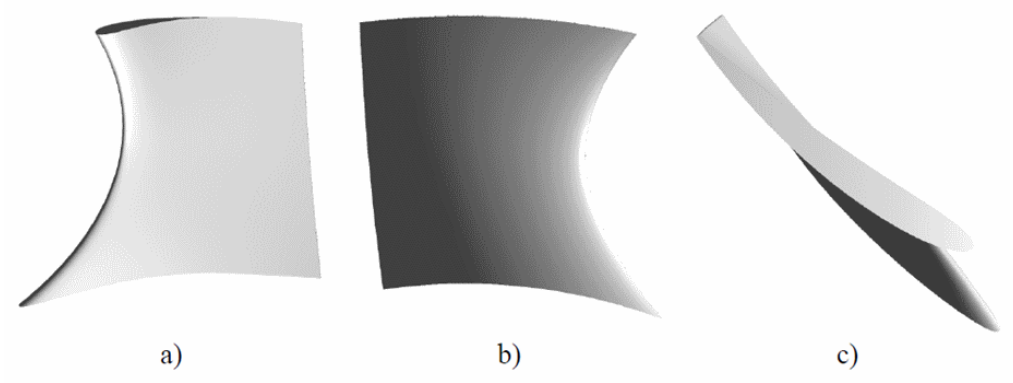

Fig. 2.2.: Views of designed swept blade (Dan26-SW)
a) tangential- (PS), b) axial-, c) from above views

2.3. Designing reversible rotor

During designing blades I realized bi-directional flow with the help of flat plate blade. The main aspect was the simple producing, harmonizing with it we haven't adjusted edge radius and inlet cone on the hub. Rounding the blade ends has happened according to decreased circle bow with tip clearance size on the blade converted to plain. The blades have been fixed by rivets on the bowed plate.

During designing I have chosen the free-vortex design (FV). In my design I have considered the blades like free-standing wings $(\sigma \ll 2)$. At calculating the blade solidity (Eck, 2003) I have used the frictionless form of force-factor. I have taken the effect of friction into account, that I take values of lift coefficient from the diagram constructed by measuring the free-standing wing-wind tunnel with consideration of glide. The Table 2.4. contains the parameters prescribed in design working point.

Table 2.4.: The input rotor design parameters of Dan007 rotor.

Parameter	**Value**
Flow coefficient (φ)	0.286
Pressure coefficient (ψ)	0.118
Revolution (n_f)	1400 min^{-1}
Outer radius (r_a)	315 mm
Blade number (N)	8
Hub to casing ratio (ν)	0.514
Designed hydraulic efficiency (η_{hT})	0.8
Tip clearance (τ)	3 mm

The main fluid flow and geometrical parameters are illustrated by Figure 2.3.

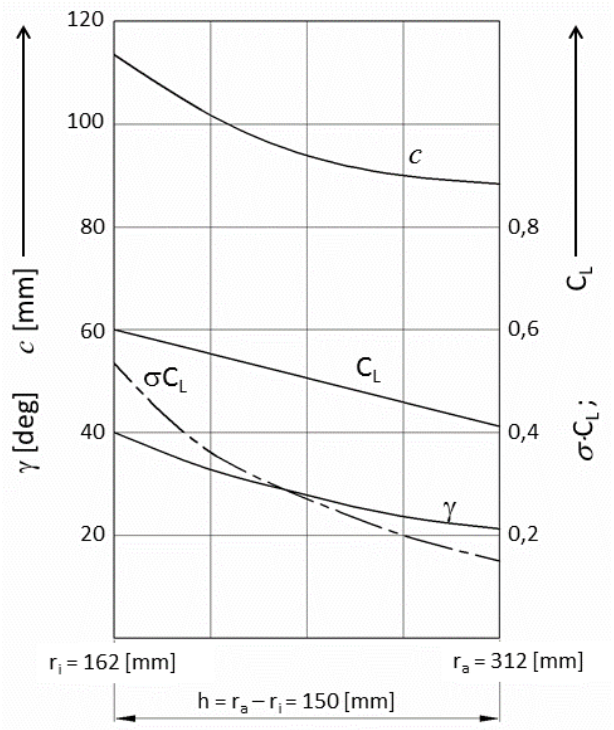

Fig. 2.3.: Important flow and geometrical parameters of Dan007 rotor

The setting up of rotor measurement test rig and evaluate of rotor characteristic were carried out in accordance with the recommendations of Gruber (1978) and Szlivka et al. (2004).

2.4. Validation of applied numerical model

For validation of my numerical model I have used Bup-26 measurement data (Vad, Bencze, 1998). I have introduced the averaged local axial flow coefficient at given radius:

$$\varphi_3\left(R^*\right)_{CFD} = \frac{v_{3m}\left(R^*\right)_{CFD}}{u_a} \tag{2.3}$$

Where the $R^* = r / r_a$ is the dimensionless radius. During the post processing I have evaluated the exit axial flow coefficient at five radial value. The evaluated results are summarized in Table 2.5.

Table 2.5.: Local axial flow coefficient $\varphi_3\left(R^*\right)_{CFD}$

$\varphi_3(0.70)_{CFD}$	=	0.4912
$\varphi_3(0.75)_{CFD}$	=	0.5203
$\varphi_3(0.80)_{CFD}$	=	0.5440
$\varphi_3(0.95)_{CFD}$	=	0.5221
$\varphi_3(0.97)_{CFD}$	=	0.4173

The Figure 2.4 represents the measured axial flow coefficient. The ±5% error band is symbolized by blue lines. It can be concluded that the results obtained from the simulation match within the measurement error with the exception of near the case ($R^* = 0.97$) because the difference here 6…7%. This mistake can be explained by the greater error of the wall-proximity and the flow effect of tip gap.

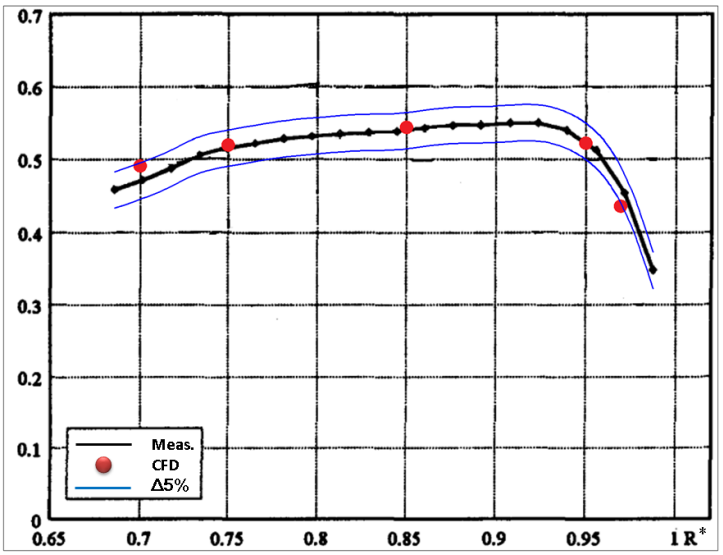

Fig. 2.4.: Simulated local axial flow coefficient measured behind Bup-26 blade (Vad, Bencze, 1998)

3. RESULTS

3.1. Rotor tip gap analyzing which designed with constant chord and diffusion number

In my subchapter I analyze the straight bladed fan (STR) with different tip clearances. The investigated tip gap series are nondimensioned by midspan chord. I listed this series of tip gap with percent format: 0.9174c_k% (1.0 mm), 1.3761c_k% (1.5 mm), 1.8348c_k% (2.0 mm), 2.2936c_k% (2.5 mm), 2.7523c_k% (3.0 mm).

3.1.1. Calculation discharge coefficient of tip gap

Discharge coefficient in the gap:

$$C_n = \frac{\overline{w}_N}{\overline{w}_{N,2D}} \tag{3.1}$$

The maximum discharge coefficient is $\tau = 1.3761 c_k\,\%$ at the tip gap size (Figure 3.1). It can be concluded that the friction loss is minimal and the average gap flow velocity has a got a maximal value here.

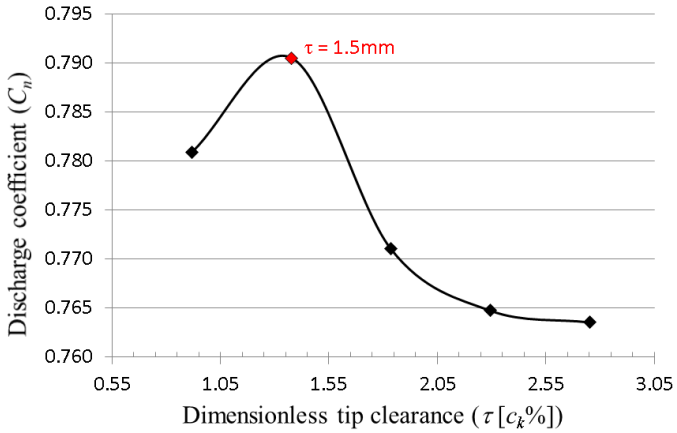

Fig. 3.1.: Discharge coefficient as function of dimensionless tip clearance

During my further investigations I give attention to the accompanying phenomenon around the $\tau = 1.3761 c_k\,\%$ clearance size.

3.1.2. Rotor hydraulic efficiency

Rotor hydraulic efficiency:

$$\eta_h = \frac{(\Delta P_t)_{CFD}}{\Delta P_t} 100 = \frac{\psi_{CFD}}{\psi} 100 \tag{3.2}$$

Local minimum can be determined at $\tau = 1.3761 c_k\,\%$ clearance size (Figure 3.2).

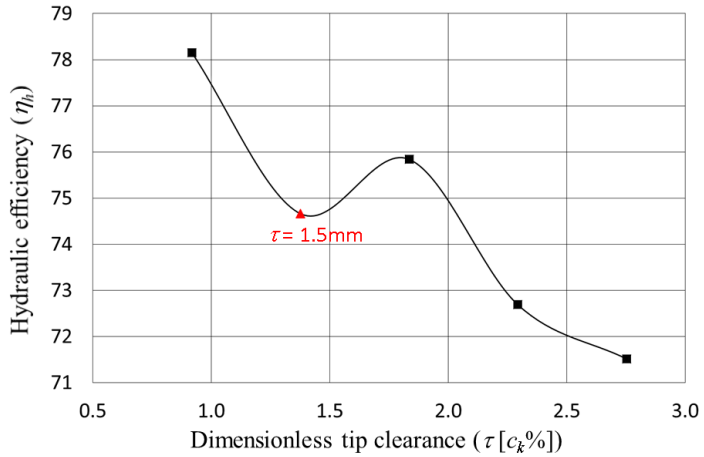

Fig. 3.2.: Hydraulic efficiency as function of dimensionless tip clearance

3.1.3. Describing 3D fluid flow with averaged parameters

Secondary velocity deviated from design condition:

$$\boldsymbol{w}_s = \boldsymbol{w}_r + \boldsymbol{w}_{sb2b} \tag{3.3}$$

Radial velocity component factor averaged on blade span:

$$Y_r = \frac{(\rho/2)\int \left|\overline{w_r}\right|^2 d\,(spn)}{(\rho/2)u_a^2} \tag{3.4}$$

Where $\left(spn = (r - r_i)(r_a - r_i)^{-1}\right)$ is the dimensionless „running" coordinate. It is obvious, the smallest radial average velocity (Figure 3.3) is given by that the largest tip gap velocity (Figure 3.1) at the gap of local hydraulically efficiency minimum (Figure 3.2) $(\tau = 1.3761 c_k\,\%)$.

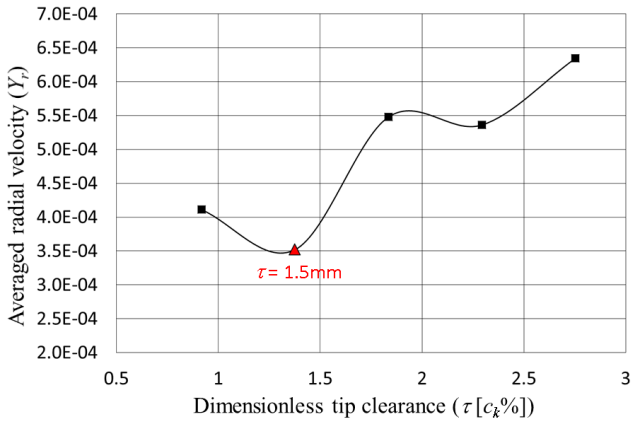

Fig. 3.3.: Averaged radially velocity component along the span

Secondary velocity component factor in designed plain:

$$Y_{sb2b} = \frac{(\rho/2)\int_0^1 \left|\overline{w_{sb2b}}\right|^2 d(spn)}{(\rho/2)u_a^2} \tag{3.5}$$

On cascade section in a determined radial plain (Figure 3.4.) I have defined the seconder component perpendicular on the designed exit relative velocity ($\boldsymbol{w}_{sb2b}$, (3.3)):

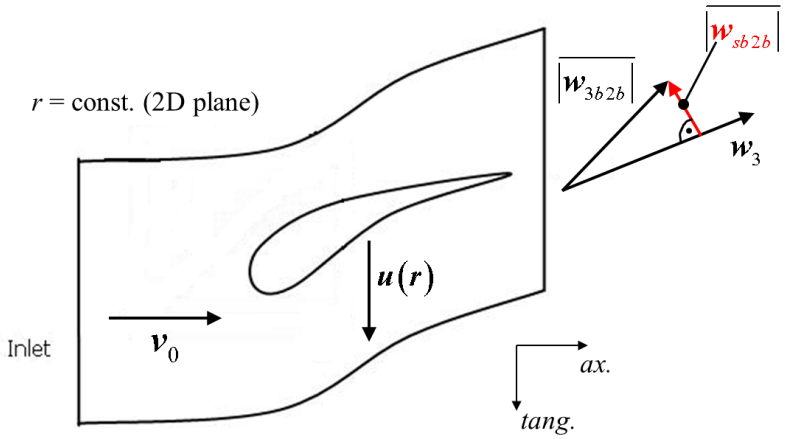

Fig. 3.4.: 3D velocity area, deviation of average projection component $\left(\overline{|w_{sb2b}|}\right)$ on 2D designed plain from designed velocity (w_3).

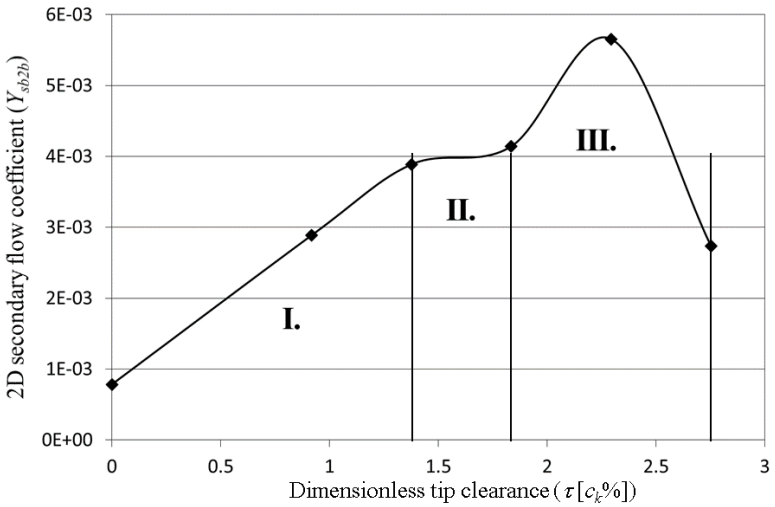

Fig. 3.5.: Secondary velocity factor averaged in designed plain as function of dimensionless tip gap.

The function of a global secondary velocity factor (Y_{sb2b}) can be partitioned into three characteristic ranges (Figure 3.5.): linear, constant and concave stages. The first one (I.) is the linear sector which is $1.3761c_k$% gap size. The second one (II.) is the constant sector as fa as $1.3761c_k$% and the last range (III.) is described by a concave function. Tip clearance of $1.3761c_k$% (1.5mm) which was given as former extrema is located at boundary between linear and constant sectors. At zero gap size the case runs together with rotor during simulation (shrouded rotor).

3.1.4. Investigation of flow blockage

The range is called „blockaged" where the analyzed axial velocity component is smaller than designed one. The value of unit function f_{ax} is one in the blocked area. Its relation can give the blockage factor with the whole flow section:

$$\mathrm{AFB} = \frac{\iint f_{ax}(r,\theta)\, r dr d\theta}{\iint 1 \cdot r dr d\theta} \tag{3.6}$$

According to Figure 3.6. I have established that the tip gap has got a local minimum $\tau = 1.3761c_k\,\%$ (1.5mm).

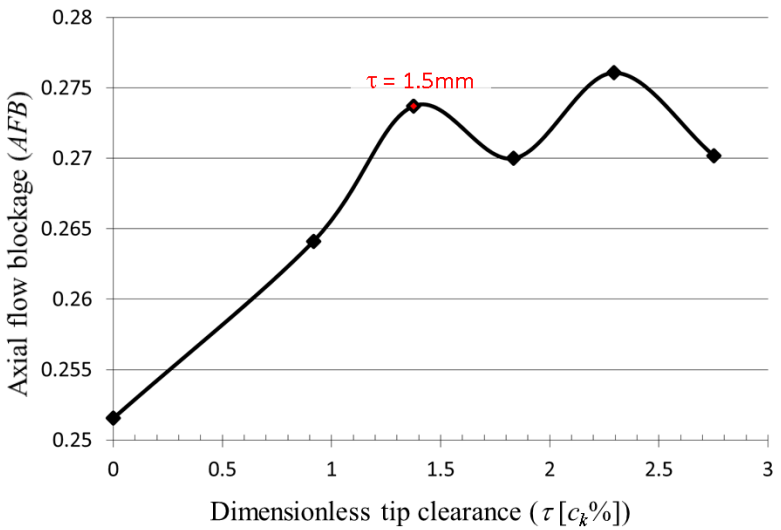

Fig. 3.6.: Axial flow blockage (AFB)

3.1.5. Static pressure distribution at blade tip

Definition of pressure coefficient:

$$C_p = \frac{p - p_0}{0.5\rho u_a^2} \tag{3.7}$$

In the direction of trailing edge the isobar lines are perpendicular on the cord in the range $\tau \le 1.3761c_k\,\%$ which is referring that clearance flow has been indicated by

blade loading here (Yamamoto, 1989). Int he direction of trailing edge at the larger investigated tip clearance $(\tau > 1.3761 c_k\%)$ the isobar lines are kinked, that is the clearance flow is influenced by viscosity in a higher degree.

In the tip gap range $\tau \geq 1.8348 c_k\%$ the pressure of entering velocity of pressure size immediately decreases, in consequence of flow section stricture (vena contracta: VC). In the case of tip gap $\tau = 1.3761 c_k\%$ (1.5mm) the vena contracta phenomena has not appeared yet (Figure 3.7.).

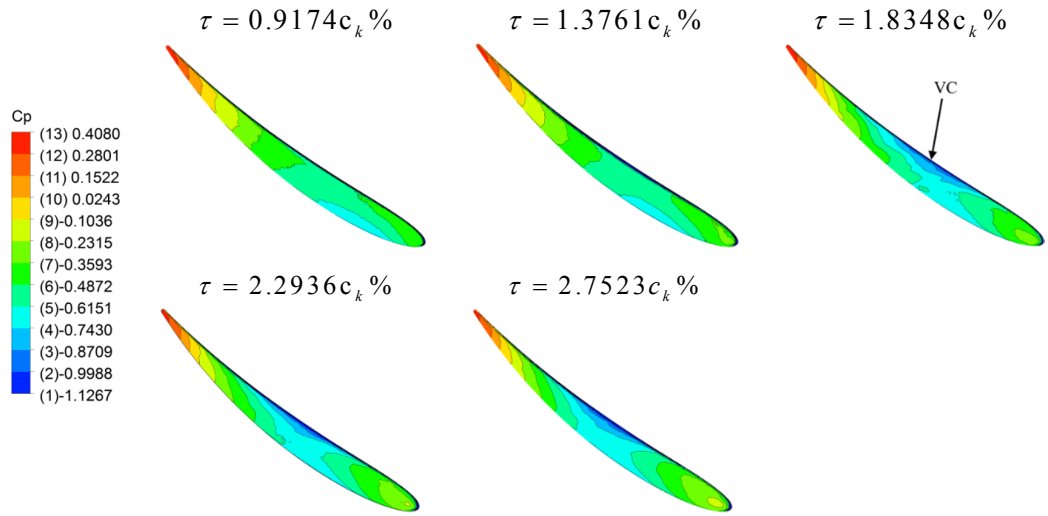

Fig. 3.7.: Static pressure coefficient distribution at the blade tip

3.2. Numerical investigation of swept blade design with prescribed design local diffusion factor method.

3.2.1. Pressure distribution along blade profile, stagnation pressure loss

At the hub and blade tip peak depression lowering can be noticed (Figure 3.8.). One of the reasons of depression decreasing is (+)SW consequence of blade tips, which results local velocity increasing. The other reason of appearing of decreased suction surface pressure gradient is the result of the smaller design diffusion number (DF):

$$DF \sim DF_{loc} = 1 - \frac{w_3}{w_{\max,free}} \Rightarrow DF \downarrow \therefore w_{\max,free} \downarrow \tag{3.8}$$

The smaller diffusion number results a smaller suction surface peak velocity $\left(w_{\max,free}\right)$:

$$p_{00} \approx p_t = p + \frac{\rho}{2} w^2_{\max,free} \approx áll. \Rightarrow w_{\max,free} \downarrow \therefore p \uparrow \tag{3.9}$$

Where (p_t) is the local stagnation pressure.

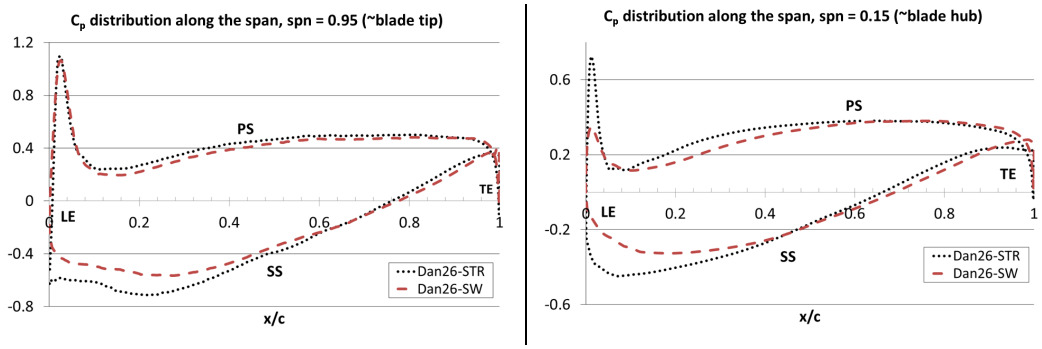

Fig. 3.8.: Pressure distribution along the profile, (C_p) figures

3.2.2. Pressure distribution in the area of blade clearance.

Distribution of pressure coefficient along of middle distance of tip clearance (Figure 3.9.).

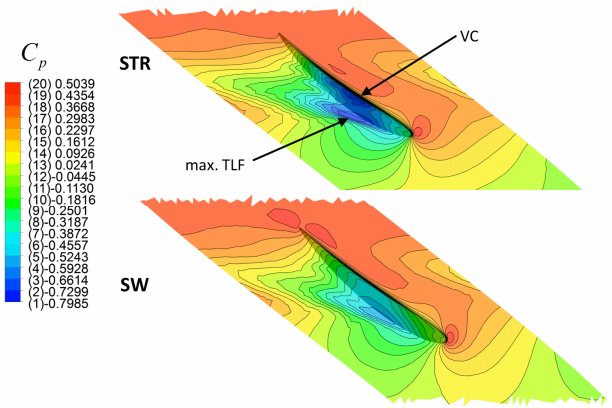

Fig. 3.9.: Distribution of pressure coefficient along of middle distance of tip clearance

In the case of the Calculating Modell given swept bladed rotor (SW) the flow loss in the gap is smaller at the investigated tip clearance ($\tau = 1.3761 c_k \%$) than in the case of straight bladed fan (STR). In the direction of trailing edge of swept blade the isobar lines are perpendicular on the cord (Figure 3.9.), which is refering that clearance flow has been indicated by blade loading here (Yamamoto, 1989). In spite of it the isobars are klinked at the straight bladed fan therefore the tip clearance flow is influenced by viscosity. A vena contracta has emerge jet at straight bladed rotor, which verifies a greater influence of viscosity. Next to the leading edge the blade profile has got a larger suction side peak depression result, that in the case of straight bladed fan the velocity of jet flow is higher and harmonizing with it the local depression is larger (Figure 3.9.), but in the case of swept bladed rotor is smaller. According to it these average velocities of flow area through to the gap have changed both in the case of reference rotor $27.05 m/s$ and in the case of swept blade $24.4 m/s$. Consequence of decreased design diffusion number is the beneficially

smaller gap velocity of swept blade which has got a moderating efficiency on blade loading. The higher discharge coefficient can verify the smaller flow loss of the swept blade in the tip clearance. $(C_n)_{SW} = 0.7884$ is at the swept blade and $(C_n)_{STR} = 0.771$ is at straight blade.

3.2.3. Investigation of streamline pattern along the plain

With the help of investigation of streamline pattern boundary layer moving and separating are can be followed and analyzed.

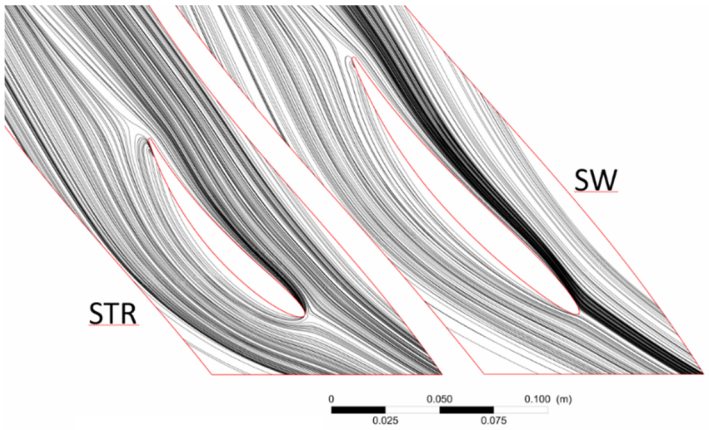

Fig. 3.10.: Presentation of streamline pattern along the borded-wall of the hub

In the case of swept rotor (SW), hub corner separation has got smaller extension than in the case of straight bladed starting rotor (STR). At the blade hub the smaller designed diffusion number (3.8) results a decreased streamline pressure gradient along the suction side (3.9). At the same time the chord lengthen and decreasing of camber angle of camber results smaller circumferential pressure changes. This is in harmony with equation (3.10) of Ng et al. (2008) bowed walls. According to these calculating model lowering of tangential and the streamline directioned pressure gradient affects against hub corner separation (Gbadebo, 2007).

$$\frac{\Delta p_{cir}}{0.5\rho w_0^2 s} = \frac{\rho w_\infty^2 2\sin\left(\frac{\Theta}{2}\right)}{0.5\rho w_0^2 c} = f(\Theta, c) \Rightarrow \left(\Theta\downarrow \wedge c\uparrow\right) \therefore \Delta p_{cir}\downarrow \tag{3.10}$$

3.2.4. Connection of velocity area blockage, radial flow and stagnation pressure increasing

Value of blockage factor is $AFB_{STR} = 27.371 \cdot 10^{-2}$ at reference blade (STR) and $AFB_{SW} = 25.5013 \cdot 10^{-2}$ at swept blade (SW). In the case of swept blade the lower axial flow blockage (AFB) has got the consequence, that its effective flow area is larger than the each rotor's, that is because of the thesis of continuity the component of axial velocity is smaller than out of blocked area. Taking in consideration the

absolute radial velocity (Figure 3.11.) at the averaged along the span is grater in he case of swept blade: the blade high is in the area from 10% to 80%, harmonizing with it tangential velocity and the angular momentum is also given larger at swept blade together with the results after simulation (Figure 3.12.).

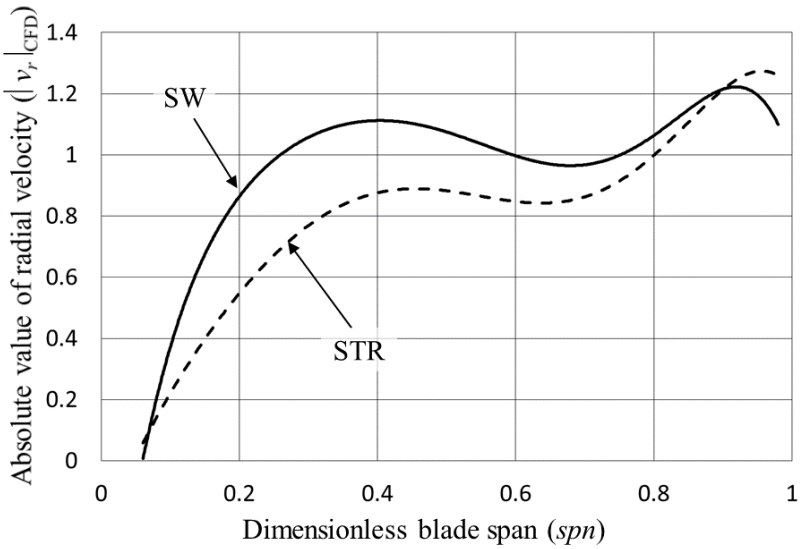

Fig. 3.11.: Distribution of radial velocity absolute value along the span

The pressure coefficient is $\psi = \Delta P_t \left(0.5 \rho u_a^2\right)^{-1}$ and flow coefficient is $\varphi = Q\left(A_{gy} u_a\right)^{-1}$. Value of Goodness Factor at this working point is $J_{MKP} = 1.04382$, in off design is $J_{Fojt} = 1.05713$. I have established, that the swept blade resulted by Calculation Modell provides increasing of a higher stagnation pressure.

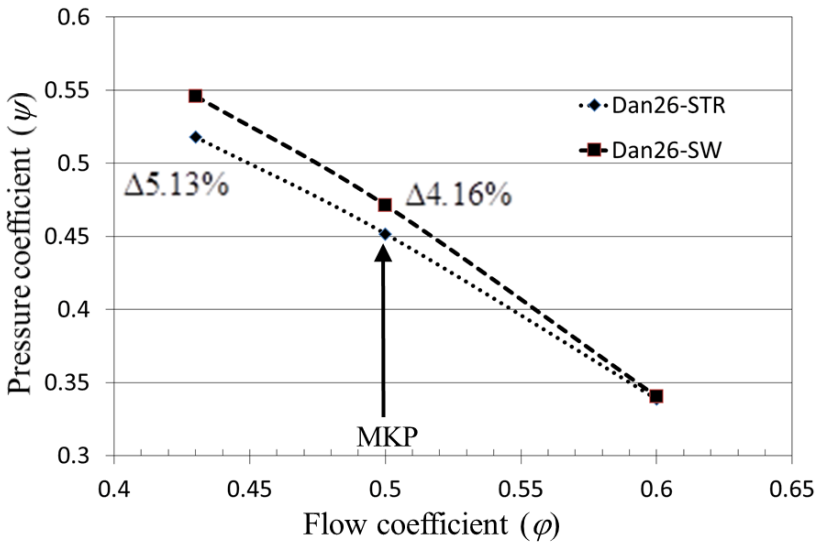

Fig. 3.12.: Characteristic by CFD simulation

3.3. Investigation of reversible rotor

The hydraulic efficiecny of is the following:

$$\eta_h = \frac{\psi_{meas}\big|_{\varphi_t}}{\psi_t} 100 = \frac{0.085}{0.12} 100 \approx 71\% \qquad (3.11)$$

I have established that the reversible rotor can only be designed for smaller region of designed pressure coefficient $0.14 \geq \psi_t$ concerning the smaller hydraulic efficiency value estimated by measure and design and taking into consideration the designed flow coefficient is comes near to stall region of characteristic (3.13. Figure). The measured hydrulic efficiency is smaller than the estimated one during calculation $\left(\eta_h < \eta_{hT}\right)$. According to this result my consequence is the following: the measured hydraulic efficiency should be estimated much lower $\left(\eta_{hT} < 0.8\right)$ because of it $\psi_{meas}\big|_{\varphi_t} \rightarrow \psi_t$. But in the case of a smaller measured hydraulic efficiency hub to tip ratio $\left(\nu \uparrow\right)$ and solidity are forming in unformable way. In the case of thick solidity the single wing model at designing has already meant a worse nearing. Taking into consideration conditions of load coefficient for free-vortex design, I have concluded that a smaller blade span is resulted in the case of a longer blade chord at hub. So grater blade twist should be realised in smaller length which can cause manufactory difficulties as well.

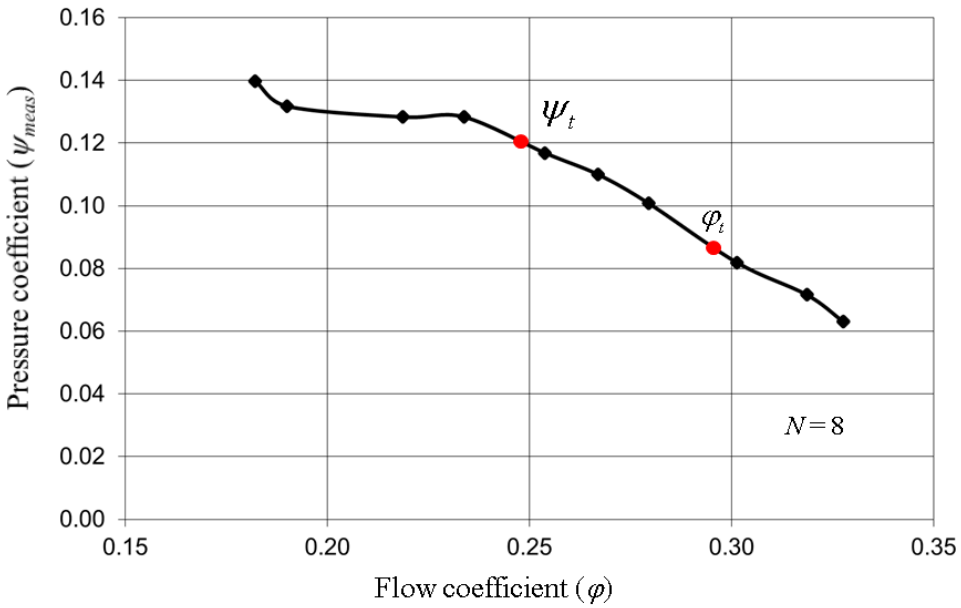

Fig. 3.13.: Characteristic of reversible rotor at designed revolution

4. NEW SCIENTIFIC RESULTS

The received and represented scientific results of my searching process are the followings:

1. With the help of CFD simulation valided by measure I have demonstrated and manifested that straight bladed fan – onto a constant chord designed by controlled vortex method and and constant diffusion number – has got a local hydraulic efficiency minimum in investigated tip clearance series. I have verified by numerical analysis, that the function of a global secondary velocity factor (Y_{sb2b}) can be partitioned into linear, constant and concave stages (Figure 1.). Besides I have verified that escorting phenomena of tip clearance belongst to local efficiency minimum are the followings:
   - In this case the discharge coefficient was given at the maximum level, that is the flow loss in the gap is the least and the smallest.
   - The radial velocity factor (Y_r) has got a global minimum.
   - The factor of axial velocity blockage (AFB) ha got a local minimum here.
   - A vena contracta in the tip gag has not emerge jet, but in the case of the larger investigated tip clearance has already been noticed.
   - The global secondary velocity factor (Y_{sb2b}) is located at the boundary of linear and constant stages.
   - In the direction of trailing edge the isobar lines are perpendicular on the cord, which is referring that clearance flow has been indicated by blade loading here. In the direction of trailing edge at the larger investigated tip clearance the isobar lines are kinked, that is the clearance flow is influenced by viscosity in a higher degree.

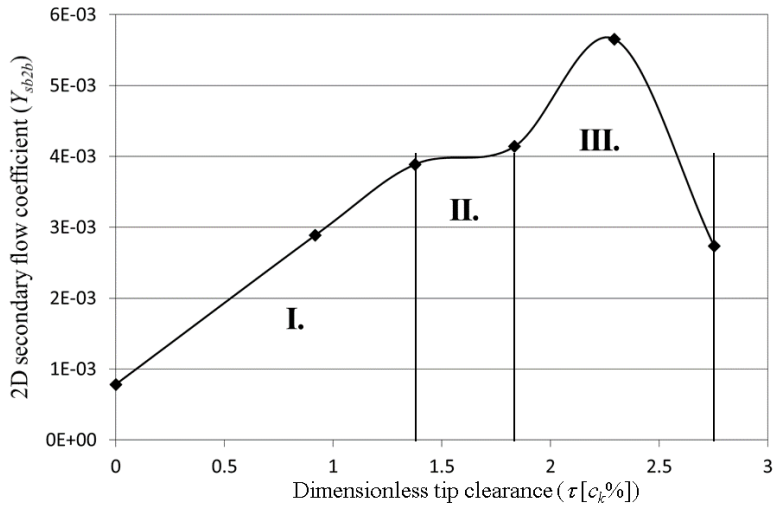

Fig. 1.: Secondary velocity factor averaged in designed plain according to function of dimensionless tip clearance

2. With the help of CFD simulation valided by measure the calculating model in the case of the Calculating Modell given by swept bladed rotor (SW) the flow loss in the gap is smaller at the investigated tip clearance $(\tau = 1.3761 c_k \%)$ than in the case of straight bladed fan (STR). In the direction of trailing edge of swept blade the isobar lines are perpendicular on the cord (Figure 2.), which is referring that clearance flow has been inducated by blade loading here. In spite of it the isobars are klinked at the straight bladed fan therefore the tip clearance flow is influenced by viscosity. A vena contracta has emerge jet at straight bladed rotor, which verifies a greater influence of viscosity. Next to the leading edge the blade profile has got a larger suction side peak depression result, that in the case of straight bladed fan the velocity of jet flow is higher and harmonizing with itt he local depression is larger (Figure 2.), but in the case of swept bladed rotor is smaller. According to the above-mentioned simulation the average velocity of flow area through to the gap is grater in the case of straight bladed fan, but it was given smaller in the case of swept blade. Consequence of decreased design diffusion number is the beneficially smaller gap velocity of swept blade which has got a moderating efficiency on blade loading. The higher discharge coefficient can verify the smaller flow loss of the swept blade in the tip clearance $\left((C_n)_{SW} > (C_n)_{STR}\right)$.

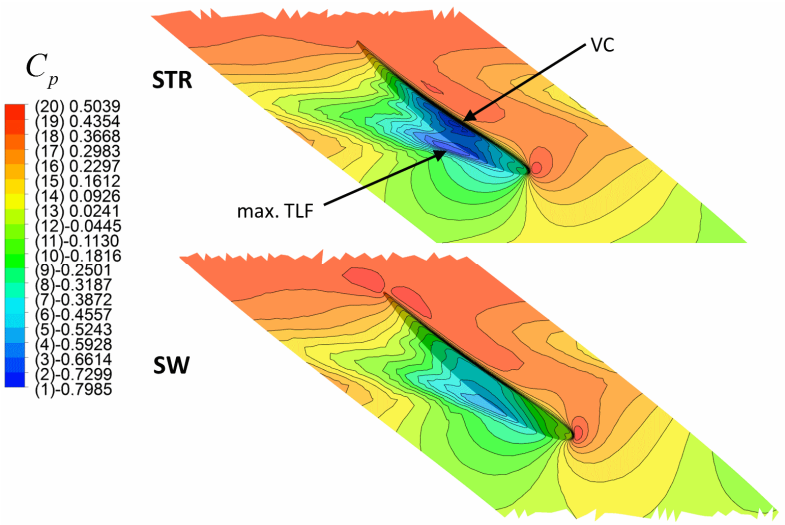

Fig. 2.: Distribution of pressure coefficient along of middle distance of tip clearance

3. With the help of CFD simulation valided by measure that the Calculating Modell has resulted the followings in the case of swept rotor, hub corner separation has got smaller extension and the enlargement of stagnation pressure is higher at designed volume flow, than in the case of straight bladed starting rotor.

At the blade hub the smaller designed diffusion number results a decreased streamline pressure gradient along the suction side. At the same time the chord lengthen and decreasing of camber angle of camber results smaller circumferential pressure changes. According to these calculating model lowering of tangential and the streamline directioned pressure gradient affects against hub corner separation.
In the case of swept blade the lower axial flow blockage (AFB) has got the consequence, that its effective flow area is larger than the each rotor's, that is because of the thesis of continuity the component of axial velocity is smaller than out of blocked area. Taking in consideration the absolute radial velocity at the averaged along the span is grater in he case of swept blade: the blade high is in the area from 10% to 80%, harmonizing with it tangential velocity and the angular momentum is also given larger at swept blade together with the results after simulation.

4. I have worked out and created a new Calculating Modell that is included constructing on increasing circulation along the radii and method of swept blade. Aerodynamically beneficial stacking line was constructed by using the Calculating Model is a non-designed character in spite of conventional designing, but an output date, which is preliminary designed result. This Calculation Modell supposes an iterative approach and a modern CFD technique. On behalf of better verifying the optimal blade geometry I have introduced the Goodness Factor.

$$J = \frac{2\pi}{Q}\int_{r_i}^{r_a} \frac{\Delta P_{t(SW)}(r)}{\Delta P_{t(STR)}(r)} \cdot v_{3m(STR)}(r)\, r dr$$

5. I have established that the reversible rotor can only be designed for smaller region of designed pressure coefficient $0.14 \geq \psi_t$ concerning the smaller hydraulic efficiency value estimated by measure and design and taking into consideration the designed flow coefficient is comes near to stall region of characteristic (3. Figure). The measured hydraulic efficiency is smaller than the estimated one during calculation $\left(\eta_h < \eta_{hT}\right)$. According to this result my consequence is the following: the measured hydraulic efficiency should be estimated much lower $\left(\eta_{hT} < 0.8\right)$ because of it $\psi_{meas}\big|_{\varphi_t} \rightarrow \psi_t$. But in the case of a smaller measured hydraulic efficiency hub to tip ratio $\left(\nu \uparrow\right)$ and solidity are forming in unformable way. In the case of thick solidity the single wing model at designing has already meant a worse nearing. Taking into consideration conditions of load coefficient for free-vortex design, I have concluded that a smaller blade span is resulted in the case of a longer blade chord at hub. So grater blade twist should be realised in smaller length which can cause manufactury difficulties as well.

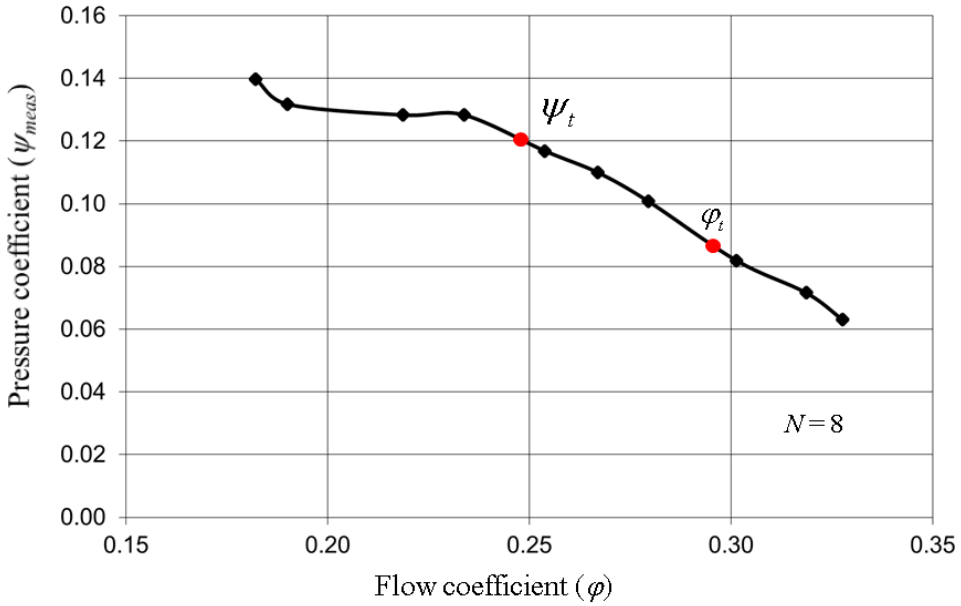

Fig. 3.: Characteristic of reversible rotor at designed revolution

5. CONCLUSIONS AND SUGGESTIONS

Considering new trends of special field of rotating machinery the aim of my thesis is creating a calculating model and its numerical investigation which takes the 3D effect and the real hydraulical efficiency into consideration during the preliminary design. My calculating model matches the controlled vortex design (CVD) with blade sweep.

The loss swept blade is lower in the blade tip clearance than the loss of preliminary reference rotor. In spite of this fact the blocked area by case behind the trailing edge is nearly the same as because of larger chord. The trailing vortex has gat a longer way for dissipation. We can see that the interaction of several parameters makes influence on goodness of blade flow. That is why I find useful to creating an optimized method of friction interblade flow with considering more multiparameter. This problem is complex because there are more local optimums and their incidental, based on a compromise and their success is not ensured that they contribute to find the global optimum (hydraulically efficiency). Local optimum aim can be eg. lower mixing behind rotor blade row, size of blocked area, streamline path on suction side of blade which is influenced by wall skin friction. The importance of some phenomenon has been balanced, that should be practically determined, in which degree the above mentioned phenomena have influence on changing of goodness factor in my thesis.

We would research some further energetical investigations of effect of higher radial flow behind swept rotor, farther from blade row, mixing loss, or flow interaction in the case of ducted diffusor behind rotor.

I have investigated the effect of different blade clearances referring to fluid for parameters, on behalf of better understanding my calculation I have introduced new parameters as well. I have establish what kind of escorting phenomenon the local hydraulically efficiency minimum has got at decreasing blade clearance. I have worked out numerical model for calculating tip clearance loss referring to analogy of discharge coefficient so I consider useful to involve these received results into the later calculating model.

I have made conclusions according to the investigation of characteristic for designing parameters of reversible flat plate blade. The property of flat plate blade, a simple hub and the blade edges are forms radius-less.

6. SUMMARY

On the basis of the technical literature I have reviewed design methods of the axial flow fans, moreover I have collected the sources of losses in turbomachinery cascade and I have analyzed their reasons. According to the technical literature imperfectness the important results of my paper are the following:

With the help of controlled vortex design method (CVD) I have designed a straight blade (STR) rotor. The rotor blades have been designed with constant chord and diffusion number. I have investigated the changing of the cascade flow parameters as a function of different tip leakage sizes. I have determined, what kind of fluid flow parameters belong to the local minimum of the global hydraulic efficiency. I have stated the global secondary speed coefficient can be divided to three specific sections.

The rotor performance and efficiency can be improved by positive sweeping of the blades. The baseline STR rotor is designed with constant chord and diffusion number. I can get the swept blade that I apply the same velocity triangles of the baseline rotor, but with different diffusion numbers (DF) at the hub and the tip of the blade. As a result of DF changing, the blade chord changes rapidly. In a consequence of it with the blade sections at hub and tip DF number we can reach an increased blade chord. The decreased DF number on both of the blade ends has result in better hydraulic efficiency. The hub and casing blade section is in combination with positive swept leading edge and unswept trailing edge. The character of swept rotor is the following, the aerodynamic stall can be reduced at the blade suction surface at the hub. From midsection to case the streamline pattern at suction surface generally overlap the primary flow field. Opposite to the baseline rotor, behind the trailing edge the 3D flow effect is stronger between the hub and the midspan. However, this 3D flow property decreases toward the blade tip in accordance with the orderly suction side streamlines of the blade. The swept rotor has been obtained with a new Computing Model, it is a result of the preliminary design process opposed to the conventional design. Namely, the new Computing Model provides the blade sweep as design output with considering of the hydraulic efficiency and 3D flow effect.

By flat-plate blade I have carried out the reversible axial flow fan. Since reversibility and flow hydraulic efficiency were investigated, the total head coefficient threshold has been given with suitable efficiency.

7. MOST IMPORTANT PUBLICATIONS RELATED TO THE THESIS

Refereed papers in foreign languages:

1. **Fenyvesi, D.**, Szlivka, F.: Design of axial flow fan rotor with constant blade chord method, Hungarian Agricultural Engineering, Gödöllő, Hungary, 2008, No. 21, pp. 23-24.

2. **Fenyvesi, D.**, Szlivka, F.: Investigation and calculation of a reversible axial flow ducted fan, Acta Polytechnica Hungarica (bírálat alatt)

3. Fenyvesi, L., **Fenyvesi, D.**: Optimization of a supporting device for mechanical harvesting, Acta Horticulturae, 2008, Nr. 768, pp. 423-430.

4. Szalay, K., Deákvári, J., Csorba, A., **Fenyvesi, D.**: Integrated ground and airbone sampling methods for measuring and modelling the change of moisture content value in agricultural lands, The Experiment, 2013, Vol. 9(2), pp. 532-540.

5. Fenyvesi, L., **Fenyvesi, D.**, Csatár, A.: Stress analysis in fruits, Advances in Mechanical Engineering, 2013, Vol. 2013, pp. 1-6.

Refereed papers in Hungarian:

6. **Fenyvesi, D.**: Axiális átömlésű reverzálható síklemez-lapátos járókerék számítása és mérési tapasztalatai, GÉP, LVII. évf., 2006, 1. sz., 14-18 o.

7. **Fenyvesi, D.**, Szlivka, F.: Síklemez-lapátos axiál ventilátor tervezése és vizsgálata, Mezőgazdaság Technika, 2012. január, 2-3 o.